

# Performance Advantages and Design Issues of SQIFs for Microwave Applications

Victor K. Kornev, Igor I. Soloviev, Nikolai V. Klenov, Timur V. Filippov, Henrik Engseth, and  
Oleg A. Mukhanov, *Senior Member, IEEE*

**Abstract**—We consider applications of SQIFs as amplifiers for gigahertz frequency range. SQIF-like structures are able to provide much higher dynamic range and linearity than a dc SQUID. We also analyze design limitations imposed by finite coupling inductances and stray capacitances. Possible ways of resolving design issues are discussed.

**Index Terms**—Josephson junctions, SQUID, SQIF, amplifiers, voltage response, high linearity, dynamic range.

## I. INTRODUCTION

FURTHER progress in wireless and satellite communications, radar and surveillance systems requires significant increase in their performance. This progress can be achieved with the development of digital receivers and transmitters capable of direct digitization and digital processing of radio frequency (RF) signals. Only superconductor ADCs can accomplish the direct digitization of high RF frequencies. Recently, a complete digital-RF receiver with a superconductor wide-band ADC implemented using robust low-temperature superconductor (LTS) Nb technology was successfully demonstrated within an operational X-band satellite ground terminal [1]. However, conventional technology antenna and low noise amplifier might limit the overall system performance by their high noise temperature and low linearity and dynamic range. One of the possible approaches to ensure the highest overall performance of the receiver systems is to use superconductor low-noise amplifier and/or antenna and their integration with the ADCs in one cryogenic system.

Both high- $T_c$  and low- $T_c$  superconductor based SQUID amplifiers were proposed and studied during last ten years [2]-[7]. However performances of these amplifiers are still far from the requirements of digital-RF systems. Despite the fact that the achieved noise temperature  $T_N \approx 1 - 2$  K [3] is quite low, dynamic range  $D = (T_{sat}/T_N)^{1/2}$  of these amplifiers is severely limited by their saturation temperature  $T_{sat}$ , which is as low as 100 - 150 K [3]-[5]. Among other problems of the

reported SQUID amplifiers is a narrow range of transfer function linearity. The use of a flux-locked-loop could noticeably increase dynamic range and linearity of amplifiers. However, an external feedback loop would limit operation frequency and bandwidth to a few tens megahertz at best, which negates their utility as amplifiers of gigahertz RF signals. It is also possible to use an internal (on-chip) negative feedback to linearize the transfer function [6], [7]. However, it is difficult to take advantage of this due to low gain of the SQUID amplifier (of order of 10-15 dB [3]-[5]).

In order to overcome these difficulties, multi-element Josephson structures including Superconducting Quantum Interference Filters (SQIF) are considered. The SQIF is an array (parallel, series, or parallel-series) of dc superconducting quantum interferometers with unconventional array structure [8]-[9]. The SQIF voltage response is characterized by a single sharp peak. Contrary to the usual optical diffraction grating which shows unique properties due to the strict periodicity of its structure, the unique properties of SQIF result just from the opposite – unconventional non-periodic array structure.

In this paper, we will consider and analyze performance advantages of SQIF structures and related design issues for implementation of amplifiers for high RF signals.

## II. PERFORMANCE ADVANTAGES OF SQIF-LIKE STRUCTURES

### A. Increase in Dynamic Range

In case of a serial SQIF of  $N$  dc interferometers (dc-SQUIDs), the thermal noise voltage  $V_F$  across the serial structure is proportional to square root of  $N$ , while the voltage response amplitude  $V_{max}(\Phi)$  and the transfer factor  $B = \partial V / \partial \Phi$  both are about proportional to  $N$ . It means that dynamic range  $D = V_{max}(\Phi) / V_F$  increases as  $N^{1/2}$ .

In case of a parallel SQIF, assuming vanishing coupling inductances ( $l = 0$ ), dynamic range is also proportional to square root of number of junctions. In fact, the thermal noise voltage  $V_F$  across the parallel structure decreases with  $N$  as square root of  $N$ , while the voltage response amplitude  $V_{max}(\Phi)$  remains constant and transfer factor  $B = \partial V / \partial \Phi$  increases as about  $N$ .

A SQIF-like structure is characterized by superior broadband frequency response from dc up to approximately  $0.1 \cdot \omega_c$ , where  $\omega_c$  is characteristic Josephson frequency [10]. Therefore the further increase in characteristic voltage  $V_c$  of Josephson junctions by implementation niobium technology with higher critical current density or by use of high- $T_c$  superconductors should extend frequency band up to several

Manuscript received 19 August 2008. This work was supported by ONR under grant RUP1-1493-05-MO via CRDF GAP and in part by ISTC grant 3743 and Russian grants on scientific schools PGSS 5408.2008.2 and PGSS 133.2008.2.

V. K. Kornev, I. I. Soloviev, N. V. Klenov and T. V. Filippov are with Moscow State University, Moscow 119991, Russia. (phone: 7-495-939-4351, fax: 7-495-939-3000, e-mail: kornev@phys.msu.ru).

H. Engseth and O. A. Mukhanov are with the HYPRES, 175 Clearbrook Road, Elmsford, NY 10523, USA (e-mail: mukhanov@hypres.com).

tens of gigahertz. Moreover, the SQIFs can be immune to a high interference which in turn decreases the amplifier saturation problem plaguing SQUID-based systems.

### B. Increase in Voltage Response Linearity

Recently we introduced a design approach based on intelligent synthesis SQUID networks. We proposed the design of multi-SQUID serial structures capable of providing periodic high linearity voltage response [11]. The approach is based on formation of the serial structures which are able to provide periodic triangular voltage response to magnetic field  $B$ . Using the interferometer cells with harmonic voltage response, one can synthesis a serial array consisting of many groups of identical interferometers, in which each group is to provide specific spectral component of the resulting voltage response of the array. According to estimations, the response linearity reaches 120 dB if number of the groups is as high as about 165. The second way for synthesis of the highly linearity array structure is implementation of differential scheme of two serial arrays of dc interferometers biased by a current  $I_b = I_C$  (critical current biasing), where  $I_C$  is the interferometer critical current.

Now, we have proposed the next generation of the one- and two-dimensional multi-element structures characterized by a SQIF-like high linearity voltage response [12]. The structures are based on the use of a differential scheme of two magnetically frustrated parallel SQIFs with both specific cell area distribution  $a(x)$  along the array and critical current biasing (see Fig. 1a). The optimal cell area distribution allows the increase of the voltage response linearity up to the levels required. This cell area optimization can be performed by numerical solution of a master equation with aid of an iterative algorithm. The problem can have more than one solution, each corresponding to a specific linearity value. One of the solutions at vanishing coupling inductances ( $l = 0$ ) follows:

$$a(x)/a_{\Sigma} = 1.2 - 0.48\sin^3(\pi x), \quad (1)$$

where  $a_{\Sigma}$  - total area of SQIF. This cell area distribution provides response linearity up to 101 dB.

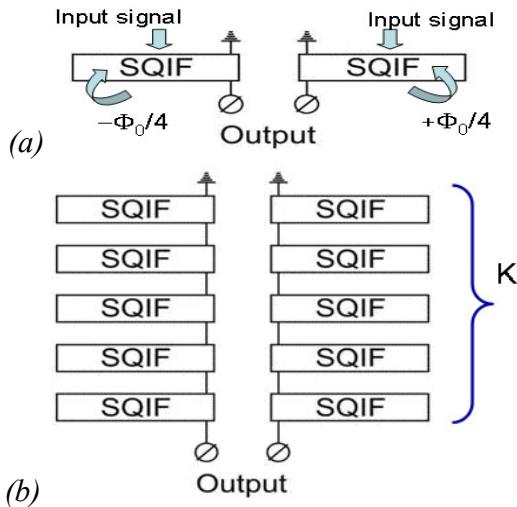


Fig. 1. (a) Differential scheme of two parallel SQIFs frustrated by  $\Phi_0/2$  and (b) two-dimensional differential serial-parallel SQIF structure.

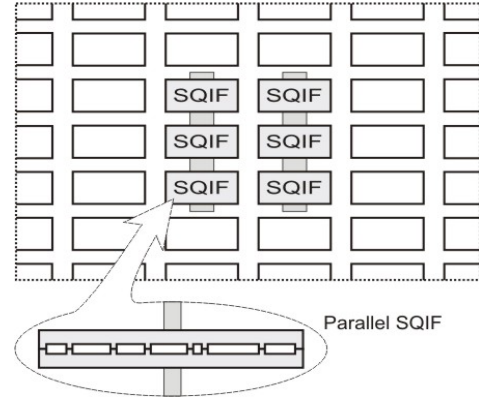


Fig. 2. Active electrically small antenna based on two-dimensional differential serial-parallel SQIF-structure (filled structure in the central part of chip). These SQIF sections are connected by strips of normal metal. The chip also contains a regular matrix of identical dummy blocks of parallel SQIFs (not-filled rectangular) to provide homogeneous magnetic field distribution in the center part of the chip. Inset shows a block with parallel SQIF. The topology of the SQIF is an example for high- $T_c$  superconductor bicrystal Josephson junction technology.

### C. Application Design Flexibility

Both the dynamic range and the output signal amplitude can be additionally increased by connection of the differential SQIF structures in series, i. e. by coming to two-dimensional differential serial-parallel SQIF structure (see Fig. 1b). The number  $K$  of the elements connected in series is responsible for output signal amplitude, while total number of Josephson junctions  $N^* = N \cdot K$  is responsible for dynamic range of the structure. Varying the number of elements connected in parallel ( $N$ ) and in series ( $K$ ), one can change impedance of the structure in wide range.

The synthesized multi-element structure can be used to develop high performance low noise amplifiers. The proposed two-dimensional structure can be also used as an active electrically small antenna (Fig. 2). The gain of such an antenna can be significantly increased by integrating with an additional flux focusing structure including even reflecting parabolic antenna. Varying the number of elements connected in parallel ( $N$ ) and in series ( $K$ ), one can set an impedance value needed to minimize a negative impact of the antenna load used.

## III. DESIGN ISSUES

The expected high performance of multi-element SQIF-like structures is based on estimations drawn for idealized structures as well as on the voltage response characteristics calculated using the Resistively Shunted Junction (RSJ) model of Josephson junction. However, the actual performance of the implemented SQIF array structures may be quite different. Below we analyze limitations imposed by finite coupling inductances and stray capacitances.

### A. Parallel Arrays: Finite Coupling Inductances

Finite (non-zero) value of coupling inductances  $l$  between Josephson junctions in parallel array has fundamental importance for all principal characteristics of the SQIF array, since it imposes limitations on coupling radius.

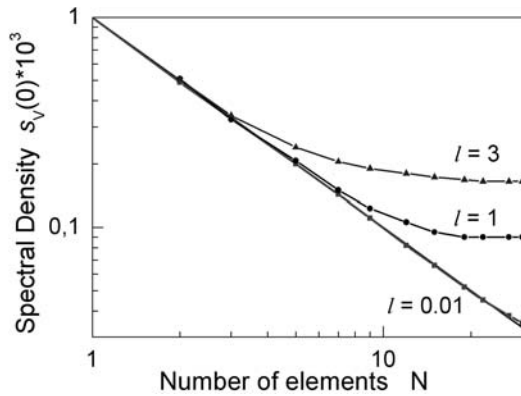


Fig. 3. Dependence of the normalized low-frequency spectral density of the resistor voltage noise on number  $N$  of resistors  $R_N$  connected in parallel by coupling inductances at different normalized values  $l$  of the inductances.

As for differential voltage response linearity, the negative influence of the inductances can be substantially reduced by shunting resistors  $R_{SH}$  connected in parallel to the inductances [12]. Due to the fact that impedance of the  $RL$  circuit becomes low enough at Josephson oscillation frequency, the parallel array voltage response approaches the one for smaller and smaller inductance with decrease of  $R_{SH}$  down to some optimal resistance value depending on the normalized inductance  $l$ ; the further increase in  $R_{SH}$  leads to some other linearity distortions. Thereby the most efficient design approach is the synthesis of an optimal SQIF structure with the cell area distribution  $a(x)$  optimized for the finite value of  $l$ . In this case one should use a high performance numerical simulation technique (e.g. software PSCAN [13]) for the calculation of the SQIF voltage response  $V(\Phi)$  in every cycle of the iterative algorithm which has to be used to solve master equation [12].

The finite coupling radius limits the increase of both dynamic range and transfer factor  $dV/d\Phi$  with the increase of number of junctions  $N$ . To study the noise characteristics in more clear and powerful manner, one can perform numerical simulation of a parallel array of the inductively coupled resistors  $R_N$  each connected to an individual source of white-noise current [13]. Fig. 3 shows dependence of the low-frequency spectral density  $S_v(0)$  of the resistor voltage noise on the number of resistors  $N$  at different values of normalized

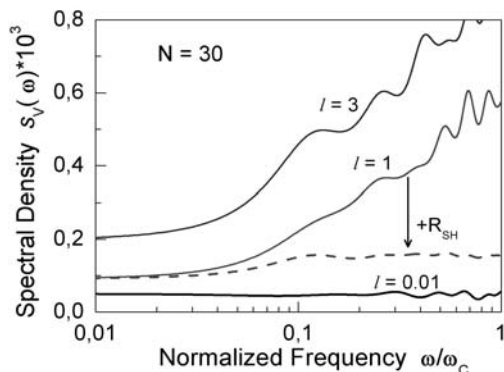


Fig. 4. Dependence of the normalized spectral density of the resistor voltage noise in parallel array of 30 resistors  $R_N$  on normalized frequency at different normalized values  $l$  of the coupling inductances. Dashed curve shows the spectral density dependence for  $l = 1$  when all the coupling inductances are shunted by noiseless resistors  $R_{SH} = 0.1R_N$ .

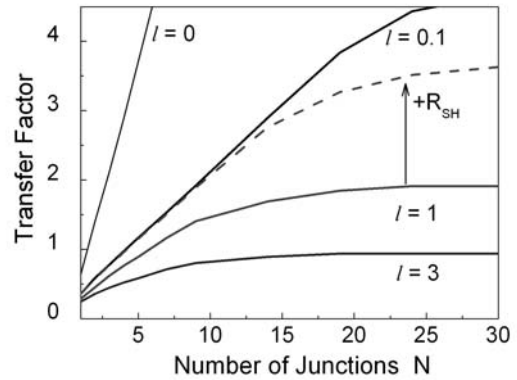


Fig. 5. Normalized transfer factor  $B = dV/d\Phi$  for parallel array of Josephson junctions versus number of junctions  $N$  at different normalized values  $l$  of coupling inductances. Dashed curve shows the transfer factor dependence for  $l = 1$  when all the coupling inductances are shunted by resistors  $R_{SH} = 0.1R_N$ .

coupling inductance  $l$ . The data are presented for the normalized frequency  $\omega/\omega_c = 10^{-3}$  well-corresponding to signal frequency range in a SQUID / SQIF amplifier (here  $\omega_c$  is characteristic Josephson frequency).

Within the coupling radius the spectral density  $S_v(0)$  decreases as  $N^{-1}$  and then it comes to a constant value when number  $N$  becomes more than coupling radius depending on  $l$ . Fig. 4 shows the spectral density  $S_v(\omega)$  versus normalized frequency ranged from 0.01 to 1 for parallel array of 30 resistors  $R_N$ . At both coupling inductances  $l = 3$  and  $l = 1$  spectral density  $S_v(\omega)$  monotonically increases with frequency and remains constant at  $l = 0.001$ . It reflects the decrease in coupling radius with frequency for both inductances  $l = 3$  and  $l = 1$ , as well as the fact that the coupling radius at  $l = 0.01$  exceeds size of the array of 30 elements in the entire frequency range.

One can see that the use of noiseless resistors  $R_{SH} = 0.1R_N$  shunting the inductances  $l = 1$  stops both the coupling radius decrease and the spectrum density increase at  $\omega/\omega_c \geq 0.1$  (see dashed line in Fig. 4). Of course the proper account of own noises of the shunting resistors will lift the curve as a whole about two times higher, as if spectral density for the noise current sources connected to basic resistors  $R_N$  becomes more by factor  $k \approx 4 - 5$ .

Fig. 5 shows dependence of the normalized transfer factor  $B = dV/d\Phi$  for parallel array of Josephson junctions versus

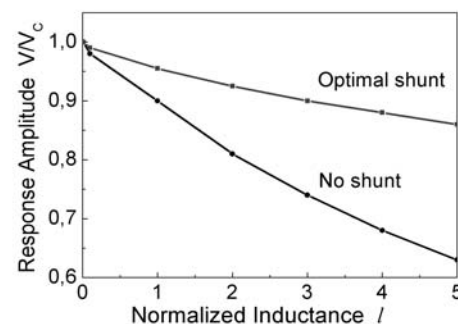


Fig. 6. The normalized voltage response amplitude  $V_{max}$  for two parallel arrays of Josephson junctions coupled correspondingly by unshunted inductances (lower curve) and by the optimally shunted inductances (upper curve) versus normalized inductance value.

number of junctions  $N$  at different normalized values  $l$  of coupling inductances. Dashed curve shows the transfer factor dependence for  $l = 1$  when all the coupling inductances are shunted by resistors  $R_{SH} = R_N$ . The observed saturation in the transfer factor dependence on  $N$  is reached when number of junctions exceeds coupling radius at frequency  $\omega/\omega_c \sim 1$ .

In conclusion, we see that the increase in dynamic range  $D = V_{max}(\Phi)/V_F$  with number  $N$  of Josephson junctions in the parallel array is severely limited by coupling radius at finite coupling inductances. Shunting of the inductances improves the linearity of the differential SQIF voltage response but does not change dynamic range in significant way. This is due to the fact that shunting increases not only voltage response amplitude  $V_{max}(\Phi)$  (as shown in Fig. 6) but also increases  $V_F$  caused by thermal noise of the shunts. Therefore, dynamic range  $D = V_{max}(\Phi)/V_F$  will likely not increase and might even decrease.

### B. Serial Arrays: Stray Capacitances

In case of an unloaded serial array of dc SQUIDs, dynamic range does actually increase with number  $N$  of interferometer cells. However in reality, parasitic stray capacitances and load impedance both are able to change substantially IV-curve of the array and hence amplitude  $V_{max}$  and the shape of the array voltage response. The decrease in  $V_{max}$  leads to the proportional decrease in dynamic range. The change in the voltage response shape degrades linearity of the entire array structure.

Fig. 7 shows typical impact of the stray capacitances on IV-curve of the serial array of dc SQUIDs. Contribution of the stray capacitance of each SQUID increases with the SQUID location from ground to signal terminal. Stray capacitances draw the IV-curve shape near the hysteretic one, as well as generate one or more peculiarities on the IV-curve. The shown peculiarity results from phase-locking phenomenon. Below this peculiarity IV-curves of the array cells do not coincide because of different "capacitive load." Above the peculiarity all the individual IV-curves coincide as a result of mutual phase-locking of Josephson-junction oscillations.

Fabrication of the serial arrays using standard niobium technology with two superconducting ground planes is

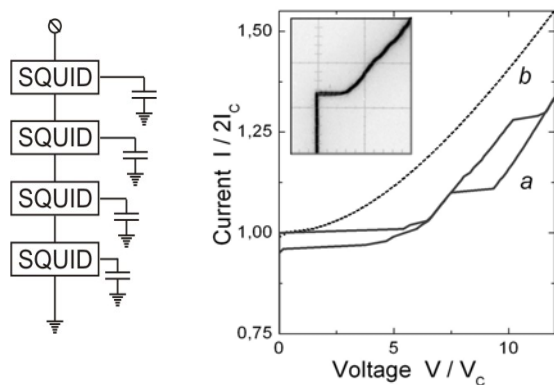


Fig. 7. Serial array with stray capacitances and typical IV curves of a serial array of 10 dc SQUIDs calculated using the RSJ model (a) in presence of the stray capacitances and (b) without capacitances. Inset shows experimentally measured IV-curve of serial array of 20 SQUIDs fabricated using niobium process.

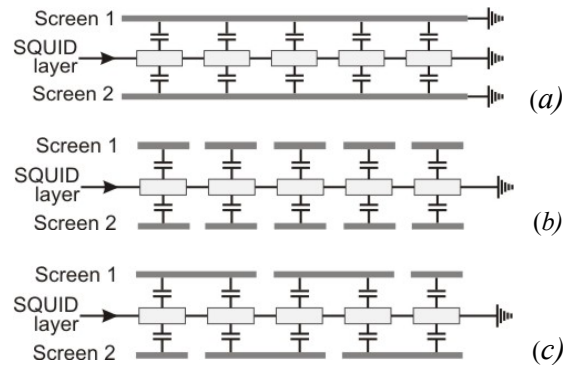


Fig. 8. Stray capacitances in SQUID array structures for fabrication using standard HYPRES niobium process with two ground plane (upper and lower planes) in cases of (a) continuous double ground plane, (b) individual double ground plane, and (c) dashed double ground plane.

accompanied by the high enough stray capacitances (see Fig. 8a). In order to decrease the stray capacitance impact significantly, one can use individual double ground plane islands for each SQUID (Fig. 8b and 8c). Both schemes are characterized by the dashed line (IV-curve "b") in Fig. 7, but the latter one provides lower inductances of the strips which connect SQUID cells.

## IV. CONCLUSIONS

Performance advantages of one- and two-dimensional SQIF-like structures for microwave applications as low noise amplifying devices come from their potential to provide increase in dynamic range with number of elements as well as highly linearity at properly optimized array structure. At the same time, there are some design limitations imposed by finite coupling inductances, stray capacitances and parasitic couplings. Therefore development of the high-performance amplifier and antenna structures needs careful and detailed design of multi-element arrays taking into consideration realistic parameters including all parasitics and couplings.

## REFERENCES

- [1] O. A. Mukhanov, D. Kirichenko, I.V. Vernik, T. V. Filippov, A. Kirichenko, R. Webber, V. Dotsenko, A. Talalaevskii, J. C. Tang, A. Sahu, P. Shevchenko, R. Miller, S. Kaplan, S. Sarwana, and D. Gupta, "Superconductor Digital-RF receiver systems," *IEICE Trans. Electron.*, vol. E91-C, No. 3, pp. 306-317, Mar. 2008.
- [2] M. Mueck, M.-O. Andre, J. Clarke, J. Gail, C. Heiden, "Radio-frequency amplifier based on a niobium dc superconducting quantum interference device with microstrip input coupling," *Appl. Phys. Letters*, vol. 72, pp. 2885-2887, 1998.
- [3] G. V. Prokopenko, S. V. Shitov, I. L. Lapitskaya, V. P. Koshelets, and J. Mygind, "Dynamic characteristics of S-band dc SQUID amplifier," *IEEE Trans. Applied Supercond.*, vol. 13, no. 2, pp. 1042-1045, 2003.
- [4] G. V. Prokopenko, S. V. Shitov, I. V. Borisenko, and J. Mygind, "A HTS X-band dc SQUID amplifier: modelling and development concepts," *IEEE Trans. Applied Supercond.*, vol. 13, no. 2, pp. 1046-1049, 2003.
- [5] G. V. Prokopenko, S. V. Shitov, I. L. Lapitskaya, S. Kohjiro, M. Maezawa, and A. Shoji, "Study of multi-channel RF amplifier based on DC SQUID for 3-5 GHz band," *IEEE Trans. Applied Supercond.*, vol. 15, no. 2, pp. 741-744, 2005.
- [6] K. D. Irwin, M. E. Huber, "SQUID operational amplifier," *IEEE Trans. Appl. Supercond.*, vol. 11, pp. 1265-1270, 2001.
- [7] M. Mueck, "Increasing the dynamic range of a SQUID amplifier by negative feedback," *Physica C*, vol. 368, pp. 141-145, 2002.

- [8] J. Oppenlaender, Ch. Haeussler, T. Traeuble, and N. Schopohl, "Sigmoid like flux to voltage transfer function of superconducting quantum interference filter circuits," *Phys. C*, vol. 368, pp. 125-129, 2002.
- [9] V. K. Kornev, I. I. Soloviev, J. Oppenlaender, Ch. Haeussler, N. Schopohl "Oscillation linewidth and noise characteristics of parallel SQIF," *Supercond. Science and Technology*, vol. 17, Issue 5, pp. S406 - S409, 2004.
- [10] V. K. Kornev, I. I. Soloviev, and O. A. Mukhanov, "Possible approach to the driver design based on series SQIF," *IEEE Trans. Appl. Supercond.*, vol. 15, no. 2, pp. 388-391, 2005.
- [11] V. K. Kornev, I. I. Soloviev, N. V. Klenov, and O. A. Mukhanov, "Synthesis of high linearity array structures," *Superconducting Science and Technology*, vol. 20, pp. S362-S366, 2007.
- [12] V. K. Kornev, I. I. Soloviev, N. V. Klenov, and O. A. Mukhanov, "High linearity SQIF-like Josephson-junction structures," *IEEE Trans. Appl. Supercond.*, this issue.
- [13] V. K. Kornev, A. V. Arzumanov, "Numerical simulation of Josephson-Junction system dynamics in the presence of thermal noise," *Inst. Physics Conf. Ser.*, IOP Publishing Ltd., no 158, pp. 627-630, 1997.